

Spontaneous chiral symmetry breaking in model bacterial suspensions

Rebekka Breier,¹ Stephan Herminghaus,¹ and Marco G. Mazza¹

¹*Max Planck Institute for Dynamics and Self-Organization (MPIDS), Am Fassberg 17, 37077 Göttingen, Germany*
(Dated: December 3, 2024)

Chiral symmetry breaking is ubiquitous in biological systems, from DNA to proteins. How do chiral structures arise from achiral interactions? We study a simple model of bacterial suspensions in three dimension that effectively incorporates active motion and hydrodynamic interactions. We perform large-scale molecular dynamics simulations (up to 10^6 particles) and describe stable (or long-lived metastable) collective states that exhibits chiral organization although the interactions are achiral. We elucidate under which conditions these chiral states will emerge and grow to large scales.

PACS numbers: 47.54.-r, 05.65.+b, 87.18.Gh, 87.18.Hf

The emergence of chiral-symmetry-breaking states in biology is still a major open question: the asymmetry of life [1]. For example, amino acids occur naturally in living beings only as left-handed enantiomers and DNA as right-handed. Bacterial suspensions also show striking examples of chiral behavior too [2].

The behavior of bacterial suspensions has attracted enormous interest, both experimental and theoretical, with the goal to unravel the physical mechanisms governing its collective states. These systems are out of equilibrium because the fluctuations are not directly coupled to external perturbations.

Here, we show that a simple model of self-propelled particles (SPP) with achiral interactions exhibits a chiral symmetry breaking with the formation of stable (or long-lived metastable) chiral dynamical states. We demonstrate how a small fraction (less than 2%) of the system in a chiral state is sufficient to cause of spontaneous organization into a chiral state that grows to mesoscopic scales.

We model bacterial suspensions through simple effective interaction among SPP that effectively mimic the active motion of bacteria. It is a common choice to choose a constant velocity v_0 for the SPP because at small Reynolds numbers rapid fluctuations of the velocity are exponentially damped. Although the SPP are polar, since they move in a specific direction, we choose an interaction that does not distinguish their orientation (i.e. a nematic interaction) which includes to leading order the effective hydrodynamic interactions among bacteria [3]. The equations of motion for particle i read

$$\dot{\vec{r}}_i = v_0 \vec{e}_i \quad (1a)$$

$$\dot{\vec{e}}_i = -\gamma \frac{\partial U}{\partial \vec{e}_i} + \vec{\xi}_i \quad (1b)$$

where \vec{r}_i and \vec{e}_i are the position and orientation, respectively, of the i -th particle, such that $|\vec{e}_i|^2 = 1$, the noise $\vec{\xi}$ is uniformly distributed on a sphere of radius η [4], and the potential that induces nematic alignment is of the

Lebwohl-Lasher form [5]

$$U = -\frac{1}{n_i} \sum_{j=1}^{n_i} (\vec{e}_i \cdot \vec{e}_j)^2. \quad (2)$$

In Eq. (2) the sum extends to the n_i neighbors of particle i within a sphere of radius ϵ . A similar potential has been studied in two spatial dimensions by a number of authors [6] [Refs], however, past work has focused on the limit of fast angular relaxation, which leads to finite-difference equations $\gamma \rightarrow \infty$. Instead, we explicitly solve Eq.(1) while leaving γ as an explicit parameter.

We perform molecular dynamics simulations of a three-dimensional system with up to $N = 10^6$ particles in a cubic box of volume $V = L^3$. We employ a velocity-Verlet algorithm with time-step $\delta t = 0.1$ for the translational and orientational dynamics [7] and implement a monotonic logical grid algorithm [8] that allows us to reach efficiently large system sizes. We employ periodic boundary conditions in all three dimensions. We show results for SPP speeds $v_0 = 0.5$, and a relaxation constant $\gamma = 0.1$. The interaction range sets the length scale in our system ($\epsilon = 1$).

Figure 1 shows the phase diagram of the system in terms of particle density $\rho = N/V$ and Péclet number

$$\mathcal{P} \equiv \frac{\text{advection}}{\text{diffusion}} = \frac{v_0 \gamma}{\epsilon \eta^2}. \quad (3)$$

At sufficiently small \mathcal{P} , the system is in a stationary state characterized by nematic order independently of ρ . As observed in [9] (but in 2D), the system is homogeneous with two sub-populations moving in opposite directions. We quantify the nematic order parameter S as the largest eigenvalue of the nematic order tensor $\mathbf{Q} = \frac{1}{2N} \sum_{i=1}^N [3\vec{e}_i \otimes \vec{e}_i - \mathbf{I}]$. As \mathcal{P} increases there is a clear transition to a homogeneous, isotropic state. The critical noise at which this transition occurs depends very weakly on γ as shown in Fig. 1(b)

In the region of the phase diagram where S is large, the system may also develop states where there is no single, global nematic director, but rather the local director forms a helical structure. Figure 2 shows

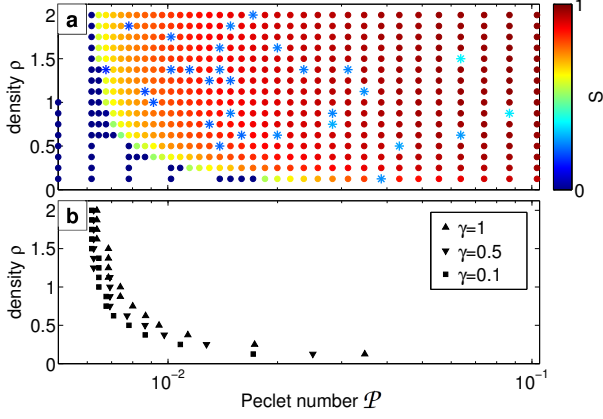


Figure 1. (a) Phase diagram of the system of self-propelled particles in terms of Péclet number \mathcal{P} and density ρ . The color indicates the global nematic order parameter. The symbols indicate different phases: * is a chiral pattern, while • are either nematic or isotropic patterns. (b) Location of the isotropic-nematic dynamic transition line for different values of γ .

some cross-sections of the system at different positions along the helical axis. The particles contained in each of these cross-sections still preserve nematic ordering, as that is the basic interaction, with a well-defined director, although fluctuations of \vec{e}_i are clearly visible (Fig. 2). As one moves along the helical axis the nematic director slowly rotates with constant twist angle. We show in Fig. 3 how the components of the local director vary along the helical axis (conventionally called x -axis). The profiles of the y and z components of the director are very well fit by sinusoidal functions, as expected for helical structures. The pitch of the helix is twice the box size L due to the nematic alignment and the periodic boundary conditions. We observe with equal probability left and right-handed helices, and, additionally, once a chiral state is formed is stable (at least up to $2 \cdot 10^6$ time steps)[10].

Following [11], we calculate the chiral order parameter

$$S_\chi = -\frac{\pi^3}{6(4-\pi)} \left\langle \left[(\vec{e}_i \times \vec{e}_j) \cdot \frac{\vec{r}_{ij}}{|\vec{r}_{ij}|} \right] (\vec{e}_i \cdot \vec{e}_j) \right\rangle \quad (4)$$

where $\vec{r}_{ij} \equiv \vec{r}_i - \vec{r}_j$, and $\langle \cdot \rangle$ represents an average performed for every particle in the system over a sphere centered on \vec{r}_i and radius $L/4$. We note that the normalization depends on the averaging radius. S_χ is a pseudoscalar symmetric for $\vec{e}_i \rightarrow -\vec{e}_i$ and vanishes in both the nematic and in the isotropic case. It is normalized so that $S_\chi = +1(-1)$ indicates left-handedness (right-handedness) of the chiral structure.

To understand the formation and (meta-)stability of the chiral structure, we test the three fundamental elastic deformations of equilibrium nematics. These deformations are described in terms of the Frank free energy

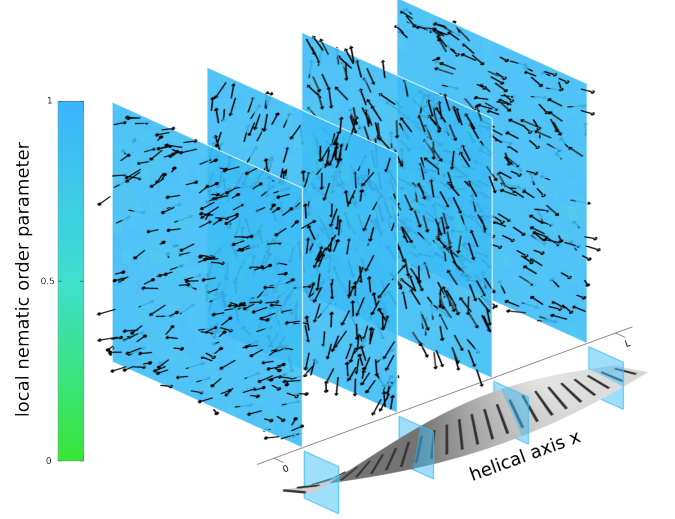


Figure 2. Cross-sections of a typical chiral configuration. The color code represents the local nematic order parameter and the little arrows represent the SPP.

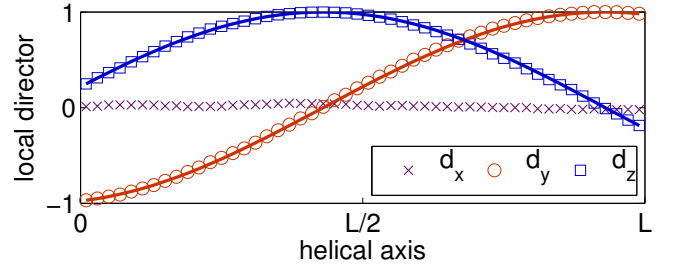


Figure 3. Components of the local director \vec{d} along the helical axis (x) of the chiral pattern (see Figure 2). The dots are the calculated components of the local director and the solid lines are sinusoidal fits $d_{y,z} = \cos(xL_{y,z}/\pi + \phi_{y,z})$.

$$\begin{aligned} F &= F_{\text{splay}} + F_{\text{bend}} + F_{\text{twist}} \\ &= \int k_1 (\nabla \cdot \vec{d})^2 + k_2 (\vec{d} \cdot (\nabla \times \vec{d}))^2 + k_3 (\vec{d} \times (\nabla \times \vec{d}))^2 dV \end{aligned} \quad (5a) \quad (5b)$$

In the continuous formulation of a director field $\vec{e}(\vec{r})$, the torque is given by

$$\vec{T}(\vec{r}_1) = \left(2\gamma \frac{1}{V_\epsilon} \int_{V_\epsilon} [(\vec{e}(\vec{r}_1) \cdot \vec{e}(\vec{r})) \vec{e}(\vec{r})] d^3r \right) \quad (6)$$

with V_ϵ being the sphere of radius ϵ around \vec{r}_1 . Because our SPP have axial symmetry only the component of $\vec{T}(\vec{r}_1)$ perpendicular to $\vec{e}(\vec{r}_1)$, $\vec{T}_\perp(\vec{r}_1)$, contributes.

The director field of a perfect twist configuration with

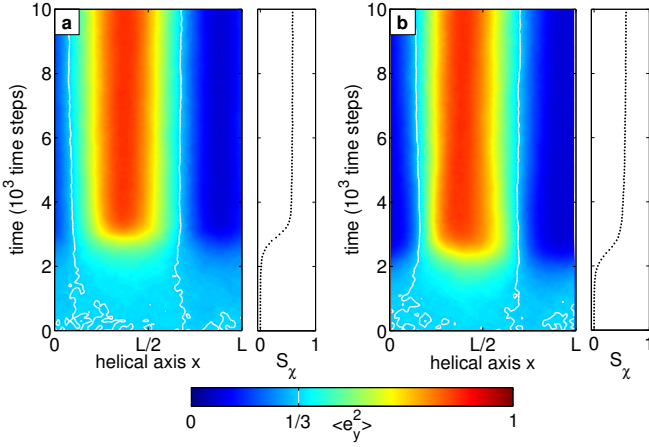


Figure 4. Time evolution of the average direction $\langle e_y^2 \rangle$ in slices perpendicular to the helical axis. (a) The system starts from an isotropic configuration and evolves spontaneously into a chiral state. (b) Seeded simulation: Isotropic configuration with 1.26% of the particles in chiral configuration.

a helical axis along the z -axis is given by

$$\vec{e}(\vec{r}) = \begin{pmatrix} 0 \\ \cos(qx) \\ \sin(qx) \end{pmatrix} \quad (7)$$

Because of the symmetry of the chiral state, we can choose $\vec{r}_1 = \begin{pmatrix} 1 \\ 0 \\ 0 \end{pmatrix}$. Using the chiral director field in the integral in Eq. (7) gives a vector parallel to $\vec{e}(\vec{r}_1)$ which results in a vanishing torque. Hence, the orientation is not changed for the next time step. As the particles are self-propelled, they propagate to

$$\vec{r}(t + \delta t) = \vec{r}(t) + v_0 \delta t \vec{e}(t) \quad (8)$$

which does not change the value of the x -coordinate and thus the description of the chiral director field still holds. Therefore, the chiral state is not changed by our model but is stable (with a sufficiently small noise value). It is easily verified that perfect bend and splay configurations produce $\vec{T}_\perp(\vec{r}_1) = 0$. This time, however, a nonvanishing $\text{vec}T_\perp$ is necessary to maintain the bend or splay configuration. Hence, the chiral state is the only stable one.

Next, we address the question how it forms. We investigate the evolution of a system with a density of $\rho = 1.625$ and noise $\eta = 0.78$ which shows a very clear chiral pattern with the helical axis denoted by x . The temporal evolution of this chiral state from isotropic is shown in Figure 4(a). The chiral structure spontaneously occurs and then grows until the full chiral is formed.

To gain insight into the early stage of the formation of the chiral structure, we look into the local fluctuations of the components of the orientation. These are defined as

$$\Delta_{e_y}^2 = \left(\langle e_y^2 \rangle - \langle e_y \rangle^2 \right) - \left(\langle e_y^2 \rangle - \langle e_y \rangle^2 \right) \Big|_{t=0}. \quad (9)$$

The fluctuations of e_y at two different times show the general behaviour (see Figure 5). In the late stage ($t = 10^4$,

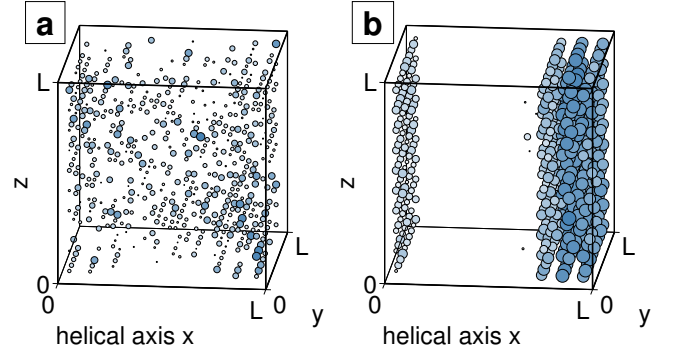


Figure 5. Fluctuations $\Delta_{e_y}^2$ at times $t = 800$ (a) and $t = 10^4$ (b) time steps. Only negative values are shown for clarity. The system is partitioned with a grid of 10^3 boxes (on average ≈ 280 particles per box).

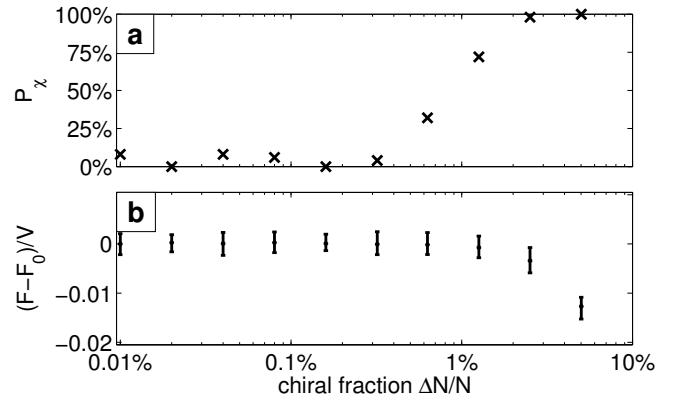


Figure 6. (a) Chiral success rate (number of chiral steady-state per seeded simulations) depending on the chiral fraction of the seeding. Fifty independent simulations are considered. (b) Frank free energy (Eq. (5), orientations coarse-grained to 10^3 boxes, numerical value of isotropic configuration removed) of scattered chiral in isotropic environment.

Fig. 5(b), one sees a clear region of negative values because the director component e_y takes low values. This feature can already be found at an early time ($t = 800$, (a)) with negative values for x close to L (especially where z is close to 0). The role of the fluctuations naturally lead to the question: How strong is the influence on the rest of the system from few particles already in the orientations corresponding to a chiral state. Therefore, we seed the system with some fraction $\Delta N/N$ in chiral order while the rest of the particles have random orientations (isotropic). The result of 50 independently seeded simulations (number of particles $N = 125000$, density $\rho = 1$, noise $\eta = 0.2$) are given in Figure 6(a). A clear transition from very few evolving chiral states (up to $\Delta N/N \approx 0.3\%$) to a success rate of close to 100% for $\Delta N/N > 2\%$ is visible. The decrease in the Frank free energy (Figure 6(b)) at the beginning of the simulations coincides with this transition.

In summary, we have shown that a model of SPP with

achiral interactions can exhibit a spontaneous chiral symmetry breaking. We demonstrate that the twist deformation

is the only stable configuration for a system of SPP. A fraction of the system as low as 2% is sufficient to produce a chiral state spanning the entire system.

-
- [1] B. Nordén, *Journal of Molecular Evolution* **11**, 313 (1978).
 - [2] E. Ben-Jacob, I. Cohen, O. Shochet, A. Tenenbaum, A. Czirók, and T. Vicsek, *Phys. Rev. Lett.* **75**, 2899 (1995).
 - [3] A. Baskaran and M. C. Marchetti, *Proceedings of the National Academy of Sciences* **106**, 15567 (2009).
 - [4] A. Czirók, M. Vicsek, and T. Vicsek, *Physica A: Statistical Mechanics and its Applications* **264**, 299 (1999).
 - [5] P. A. Lebowitz and G. Lasher, *Physical Review A* **6**, 426 (1972).
 - [6] F. Peruani, A. Deutsch, and M. Bär, *The European Physical Journal Special Topics* **157**, 111 (2008).
 - [7] J. M. Ilnytskyi and M. R. Wilson, *Computer physics communications* **148**, 43 (2002).
 - [8] S. Weinketz, *Computer Physics Communications* **74**, 228 (1993).
 - [9] F. Ginelli, F. Peruani, M. Bär, and H. Chaté, *Physical Review Letters* **104**, 184502 (2010).
 - [10] We tested the effect of different random number generators on the stability and reproducibility of the chiral state including a Mersenne twister algorithm [12]. Both the structure of a single chiral configuration (homogeneous director twist, pitch of twice the box size) as well as the overall occurrence in the phase diagram and long-lived stability remained the same.
 - [11] R. Memmer, *Liquid Crystals* **27**, 533 (2000).
 - [12] M. Matsumoto and T. Nishimura, *ACM Trans. Model. Comput. Simul.* **8**, 3 (1998).